



Contents lists available at ScienceDirect

Environmental Pollution

journal homepage: www.elsevier.com/locate/envpol

A distributed network of low-cost continuous reading sensors to measure spatiotemporal variations of PM_{2.5} in Xi'an, China

Meiling Gao^{a,*}, Junji Cao^b, Edmund Seto^c^a Environmental Health Sciences Division, School of Public Health, University of California Berkeley, 50 University Hall #7360, Berkeley, CA 94720, USA^b Key Laboratory of Aerosol Science & Technology, SKLLQG, Institute of Earth Environment, Chinese Academy of Sciences, 10 Fenghui South Road, High-tech Zone, Xi'an, 710075, China^c Environmental and Occupational Health Sciences, School of Public Health, University of Washington, 1959 NE Pacific St., Seattle, WA, USA

ARTICLE INFO

Article history:

Received 14 August 2014

Received in revised form

6 January 2015

Accepted 11 January 2015

Available online 23 January 2015

Keywords:

Low-cost portable sensor

PM_{2.5}

Network monitoring

Air quality

Exposure assessment

ABSTRACT

Fine particulate matter (PM_{2.5}) is a growing public health concern especially in industrializing countries but existing monitoring networks are unable to properly characterize human exposures due to low resolution spatiotemporal data. Low-cost portable monitors can supplement existing networks in both developed and industrializing regions to increase density of sites and data. This study tests the performance of a low-cost sensor in high concentration urban environments. Seven Portable University of Washington Particle (PUWP) monitors were calibrated with optical and gravimetric PM_{2.5} reference monitors in Xi'an, China in December 2013. Pairwise correlations between the raw PUWP and the reference monitors were high ($R^2 = 0.86\text{--}0.89$). PUWP monitors were also simultaneously deployed at eight sites across Xi'an alongside gravimetric PM_{2.5} monitors ($R^2 = 0.53$). The PUWP monitors were able to identify the High-technology Zone site as a potential PM_{2.5} hotspot with sustained high concentrations compared to the city average throughout the day.

© 2015 The Authors. Published by Elsevier Ltd. This is an open access article under the CC BY-NC-ND license (<http://creativecommons.org/licenses/by-nc-nd/4.0/>).

1. Introduction

The past few decades of rapid economic growth in China has led to increased emissions of ambient air pollution from increased motorization, urbanization, and energy consumption (Kan et al., 2012). Ambient air pollution is a growing health burden for China's population of 1.35 billion as the country's fourth largest health risk and has been estimated to result in 1.2 million premature deaths in 2010 (Yang et al., 2013). The increased focus on the health effects of ambient fine particulate matter (PM_{2.5}) has led to new policies aimed at controlling ambient air pollution. Stricter emission standards, cleaner fuels, relocation of polluting industries, and rezoning efforts have led to some improvements in air quality (Kan et al., 2012). However, China still ranks globally as one of the countries with the worst air pollution.

Effective management of air pollution is limited by sparse monitoring networks, and the high investment costs of running and maintaining monitoring sites hinder the ability to increase

coverage and quality of air pollution data (Briggs et al., 1997). Routine monitoring of PM_{2.5} recently began in China in 2012, but current regulatory networks fail to capture spatiotemporal variations in air pollution exposures that can occur due to local emissions sources such as urban transportation and finer scale meteorology, which limits the ability of regulatory agencies to identify at risk or vulnerable populations, control relevant emissions that contribute to exposures, and protect public health.

Effective management is particularly difficult in sprawling Chinese cities. Filter-based integrated instruments mask temporal patterns while continuous monitoring instruments are expensive and limit spatial coverage. In Xi'an, China only ten PM_{2.5} regulatory monitoring stations exist with six urban districts that cover an area of 833 km² (Statistical Bureau of Shaanxi Province, 2010). Yet, new lower-cost continuous monitoring instruments for PM_{2.5} are available, which can potentially fill in gaps in the regulatory monitoring network to enhance understanding of pollution hotspots. Previously, an affordable portable optical aerosol sensor, the Shinyei PPD42NS was calibrated with reference instruments in an urban area of the United States, and its measurements were found to be highly correlated with monitoring conducted by a regulatory agency and with other optical instruments (Holstius et al., 2014). At

* Corresponding author.

E-mail addresses: mcao@berkeley.edu (M. Gao), cao@loess.llqg.ac.cn (J. Cao), eseto@uw.edu (E. Seto).

lower concentrations present in the U.S., approximately linear relationships were found between the sensor's response and a U.S. EPA Federal Equivalent Method instrument (MetOne Instruments BAM-1020) and other instruments (TSI DustTrak and GRIMM 1.108). However, there is limited understanding of how the same low-cost PM sensor performs in high concentration environments that exist in China. Further, the previous study was primarily concerned with sensor calibration, and only deployed these instruments at a single fixed site.

This paper focuses on a simultaneously distributed deployment of these monitors in Xi'an, China to (1) evaluate the performance of low-cost sensors in high concentration environments against other reference instruments, (2) demonstrate the benefits of using affordable continuous monitors to identify at risk areas or populations, and (3) test the ability of these instruments to capture spatiotemporal variability across a range of environments to inform more targeted emissions reduction policies.

2. Materials and methods

2.1. Study area

As the capital of Shaanxi province and the largest city in northwestern China with almost 8.5 million residents, Xi'an is a major city in the expansion and development of central and western China (Statistical Bureau of Shaanxi Province, 2010). Xi'an also has one of the worst air pollution records in China (HEI 2010). In the last ten years (2003–2013), the annual average PM_{2.5} concentration of 167 $\mu\text{g}/\text{m}^3$ was 4.8 times China's annual standard (35 $\mu\text{g}/\text{m}^3$), 14 times U.S. EPA's annual average standard (12 $\mu\text{g}/\text{m}^3$), and 17 times WHO's standard (10 $\mu\text{g}/\text{m}^3$) (Cao, 2014). From 2004 to 2012, Xi'an met China's daily PM_{2.5} standard (75 $\mu\text{g}/\text{m}^3$) only 11.6% of the time. Although annual PM_{2.5} levels have decreased over the last decade from 192.5 to 158.1 $\mu\text{g}/\text{m}^3$, Xi'an air pollution problems are exacerbated by terrain and meteorology, reliance on coal burning, urban growth, and increased motorization. Xi'an's location in the Yellow River Basin, low wind speeds (45% of the time in the winter with no wind), and little precipitation in the winter exacerbates air quality issues by limiting natural dispersion of pollutants (Cao, 2014).

2.2. The PUWP monitor

We developed the Portable University of Washington Particle (PUWP) monitor, which consists of a low-cost PM sensor (Shinyei PPD42NS, \$15 USD) that measures particle counts based on the principle of light scattering, a microprocessor, real-time clock, data logger, and temperature and relative humidity sensor, and a small LED display (Fig. 1). The specifications of the Shinyei sensor are

Table 1

Descriptions of sampling sites in the distributed sensor network.

Site	Type	Environment	Sampling height (m)	Distance to major road ^a (m)	Type of traffic
A	Urban Residential	Medium-rise housing within old city walls, tree-lined roads	10	255	Medium
B	Urban Residential	Gated medium-rise housing near subway construction	3	105	Heavily congested
C	University	Quiet, tree-lined campus near 2nd ring road	3	242	Congested
D	University	Quiet, tree-lined campus near 2nd ring road	3	476	Congested
E	Village	Quiet residential, Near new high rise developments under construction	13	1150	Light
F	Village	Quiet residential, near 3rd ring road	3	828	Light
G	Office Building	Mix of office buildings, residential high rises, and parks	10	66	Congested
H	Public Library	Heavily trafficked area with street vendors and 2nd ring road and major corridor	10	72	Heavily congested

^a Major roads include highways, ring roads, major arterials in the east–west and north–south direction.

described in the manufacturer's datasheet (Shinyei Corp. 2010), which indicate that it is designed to sense particles primarily 1 μm in diameter. The sensor is sampled by the microprocessor according to the manufacturer's specifications, continuously over a 30-s interval, which produces a raw uncalibrated sensor signal (low pulse occupancy time). The only calibration data provided by the manufacturer's datasheet is for cigarette smoke particle count concentration. Based on these data, there is an approximate error of 25% in particle measurement across most of the sensor's range. At very low concentrations, the error becomes substantial (e.g., over 50% error below 100,000 particles per cubic feet). For outdoor ambient monitoring applications, the sensor's raw signal must to be calibrated with co-located reference instruments to obtain mass concentration measurements. The calibration and performance of the Shinyei PPD42NS has been previously described for lower ambient air concentrations found in the U.S. (Holstius et al., 2014), but is reassessed in this study for the different particle composition and higher concentrations found in Xi'an. Although the PUWP monitor is designed to operate on a rechargeable lithium polymer battery, for this study, all monitors were connected to 240 V wall outlet power because outlet power was readily available and because this was a pilot study, resources were not available to change the batteries for the PUWPs deployed at more remote



Fig. 1. The Portable UW Particle (PUWP) monitor (left), and internal components (right).

sampling sites. The battery allows it to continue to operate during short-term power outages. Larger batteries can be used to provide greater protection from outages as necessary.

2.3. Field deployment

2.3.1. Calibration of sensors

To calibrate the raw sensor readings from the PUWP monitors, and to assess between-monitor variations, seven PUWPs were co-located alongside an optical instrument (TSI DustTrak II Model 8532) equipped with a PM_{2.5} impactor, 24 h gravimetric filter measurements (Airmetrics MiniVol Tactical Air Sampler) of PM_{2.5}, and an hourly beta-attenuation monitor (MetOne Instruments E-BAM). During the calibration phase, the PUWP monitors, DustTrak, E-BAM, and MiniVol were co-located on the roof of the Institute of Earth Environment Chinese Academy of Sciences (IEECAS) in Xi'an, China from December 16 to 20, 2013.

MiniVol filters were changed daily between 8 and 10am. PM_{2.5} filters (47 mm Whatman quartz microfiber) for the MiniVols were pre-heated at 900 °C for 3 h before sampling to remove carbon contamination. Exposed filters were stored in a 4 °C refrigerator before analysis to minimize evaporation of volatile components. All pre- and post-sampling filters were weighed using a Sartorius MC5 electronic microbalance with $\pm 1 \mu\text{g}$ sensitivity. Filters were reweighed until the differences between replicate weights were less than 20 μg and less than 10 μg for samples and for blanks, respectively. Replicate weights were then averaged to represent the pre- and post-sampling mass of the filters. Mass concentrations were calculated from dividing the net change in mass by the total volumetric flow during the sampling time of each filter.

The DustTrak data from the calibration phase were adjusted using the gravimetric MiniVol results to account for humidity effects and local PM composition. The DustTrak was co-located with a MiniVol measuring 24 h samples of PM_{2.5} during the four day calibration phase. DustTrak PM_{2.5} measurements were time-matched with the start and end sampling times of the co-located

MiniVol for each of the four 24 h samples. The resulting ratio of the MiniVol-DustTrak 24 h PM_{2.5} mass concentration from the DustTrak was used to adjust the 1 min DustTrak PM_{2.5} data.

Because the DustTrak was able to give higher time-resolution PM_{2.5} mass concentrations, we decided to use the MiniVol-corrected DustTrak as the reference instrument in this study. After correcting DustTrak data using co-located MiniVol mass concentrations, we established a calibration relationship between each PUWP's raw sensor readings and the PM_{2.5} mass concentration from the DustTrak.

Pairwise plots between the instruments' were compared after smoothing data using 1 min and hourly averages. Coefficients of determination (R^2) were used to assess the strength of linear correlations. Based on evidence of a non-linear sensor response at middle to high concentrations, polynomial regression was used to model the relationship between each PUWP's raw sensor values and mass concentration measurements obtained from the co-located DustTrak. We also examined the effects of including temperature and relative humidity in the models. The number of terms in the polynomial models was assessed using the Bayesian information criterion (BIC) and standard error of the regression (S) to select the best fit model for each PUWP. A predictive model was selected for each PUWP monitor.

2.3.2. Distributed sensor network

To assess concentrations at different sites in Xi'an, we established a network of eight locations across Xi'an, which were monitored from December 9 to 16, 2013. The eight sites were located in residential, commercial, governmental, and academic areas and were varying distances from major roads with different types of traffic intensities during the day (Table 1). The sampling heights (3–13 m) also varied to find a safe, accessible location for the devices. At each site, one PUWP monitor was co-located with a MiniVol that collected 24 h filter measurements of PM_{2.5}. MiniVol filters were changed daily between 8 and 10am. Sites were selected to capture environments with varying sources and conditions

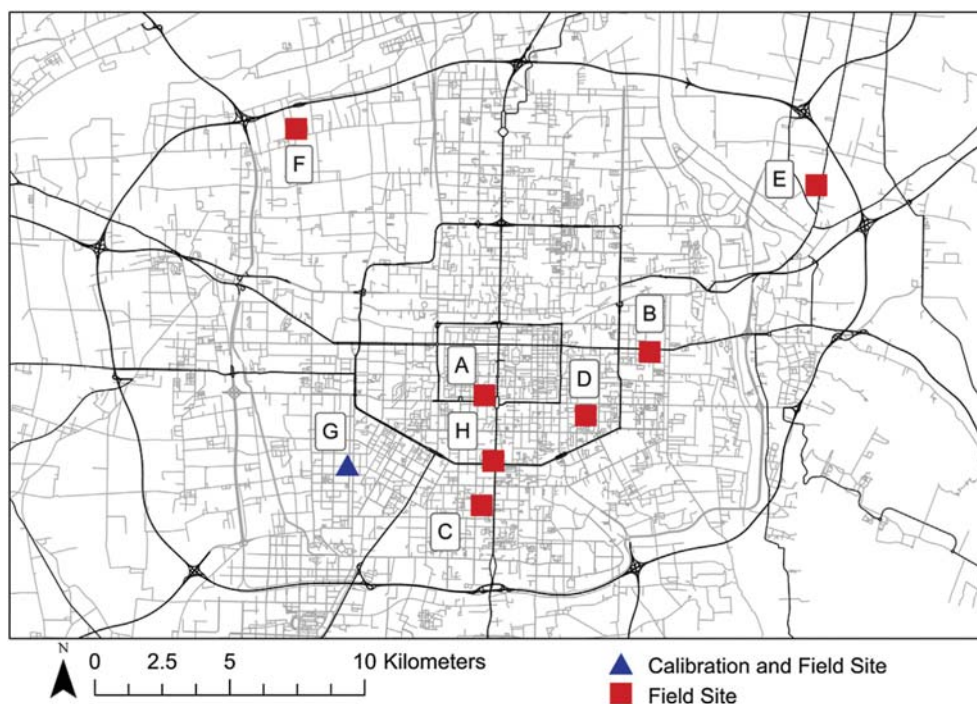


Fig. 2. Map of calibration and field sampling sites in Xi'an, China.

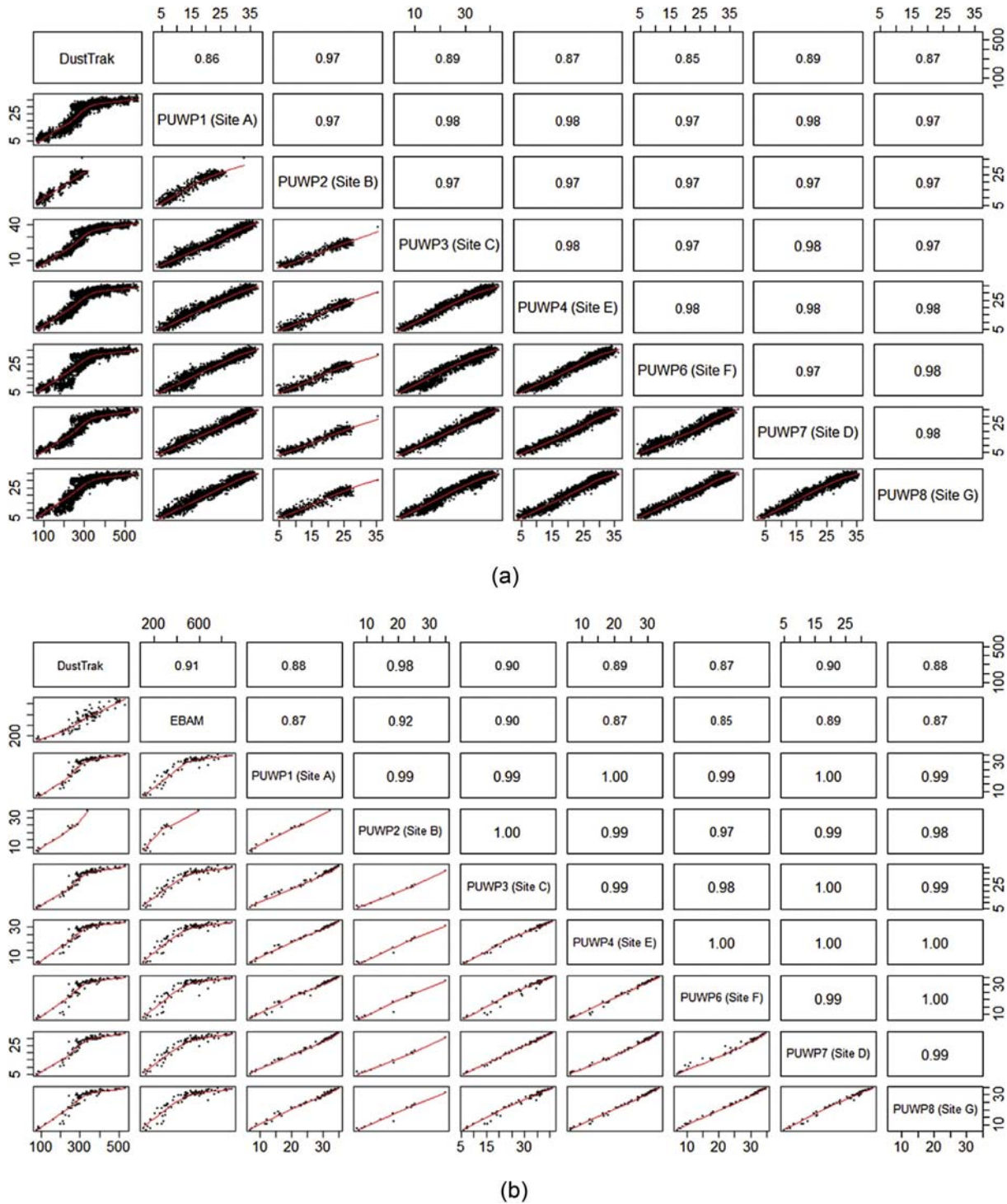


Fig. 3. Pairwise correlations between (a) 1 min averaged PUWPs and DustTrak data and (b) 1 h averaged PUWPs, DustTrak ($\mu\text{g}/\text{m}^3$), and E-BAM ($\mu\text{g}/\text{m}^3$) data at co-located site from December 16 to 20 December 2013. In both Fig. 3(a) and (b), raw sensor (low pulse occupancy) units are shown for the PUWPs. Loess smoothers are superimposed on pairwise plots. PUWP5 (Site H) was excluded because the sensor was lost.

typical of a Chinese city. Sites included (A–B) residential neighborhoods, (C–D) university campuses, (E–F) villages, (G) a building in Xi'an High-technology Zone (location of IEECAS, where the calibration described in 2.3.1 was conducted), and (H) public library near a busy intersection (Fig. 2).

Raw sensor data from each of site's PUWP was converted to a time series of 1 min mass concentrations using the PUWP's

corresponding best-fit calibration model derived during the calibration phase. This time series was further aggregated into 24 h averages, which were then compared to the 24 h integrated mass concentration measurements from each site's MiniVol using coefficients of determination (R^2). Aside from 1 min to 24 h averaging, which provides some low-pass filtering and smoothing of outliers, no other signal processing was applied to the data.

Table 2a

Predictive models comparison using Bayesian information criterion (BIC). A lower BIC when comparing two models for the same data indicates a better fitting model while accounting for complexity of the model. All models had significant ($P < 0.001$) relative humidity (RH %) and temperature (T °C) terms. Model with lowest BIC is marked with an asterisk (*) for each PUWP.

Model ^a	Bayesian information criterion (BIC)						
	PUWP1 (Site A)	PUWP2 (Site B)	PUWP3 (Site C)	PUWP4 (Site E)	PUWP6 (Site F)	PUWP7 (Site D)	PUWP8 (Site G)
Linear	58,888	7094	57,649	58,368	59,103	57,945	58,673
Linear with RH and T	58,522	7082	57,435	58,271	58,789	57,650	58,484
3rd Order Polynomial	57,530	7039	55,641	57,146	57,681	55,962	57,292
3rd with RH and T	57,546	6906	55,397	57,159	57,649	55,852	57,274
4th Order Polynomial	57,021	7022	54,889	56,697	57,366	55,374	56,831
4th Order with RH and T	56,578	6887*	54,829	56,188	56,460	55,193	55,785
5th Order Polynomial	57,028	6969	54,897	56,704	57,368	55,369	56,837
5th Order with RH and T	56,559*	6893	54,827	56,164	56,422*	55,141	55,764*
6th Order Polynomial	57,017	6969	54,897	56,687	57,375	55,342	56,845
6th Order with RH and T	56,564	6899	54,759*	56,160*	56,430	55,124*	55,772

^a All models were specified to have an intercept of zero.

To test if integrated PM measurements could be misclassifying or masking differential exposures, we compared the mean concentrations from the PUWP monitors to each site's MiniVol measurements, to determine if the sites rank ordered in the same manner regardless of instrument, and quantified the presence of extreme values, defined as more than 1 standard deviation from the city-wide mean of the MiniVol mass concentrations across all the sites for that day. A standard deviation above the city-wide average concentration was chosen as the threshold for comparison because 24 h PM_{2.5} conditions in Xi'an exceeded existing health standards. For reference, 24 h PM_{2.5} concentrations standards have been set at 25 and 35 $\mu\text{g}/\text{m}^3$ by the World Health Organization (World Health Organization, 2005) and the U.S. EPA (US EPA, 2012), respectively.

3. Results

3.1. Calibration phase PM concentration, relative humidity, and temperature

The 1 min DustTrak PM_{2.5} measurements averaged 328.3 (range: 66.6–563.7 $\mu\text{g}/\text{m}^3$), hourly E-BAM PM_{2.5} concentrations averaged 485.0 $\mu\text{g}/\text{m}^3$ (range: 77.0–889.0 $\mu\text{g}/\text{m}^3$), and 24 h integrated PM_{2.5} concentrations from the MiniVol ranged from 330.47 to 413.45 $\mu\text{g}/\text{m}^3$. Relative humidity averaged 6.1% (range: 3.2–16.9%) and temperatures averaged 11.4 °C (range: –3.5–19.2 °C).

3.2. Calibration phase PUWP raw correlations with DustTrak and E-BAM

Under the high ambient PM_{2.5} concentrations observed in Xi'an, China, the PUWPs performed well against the commercially available reference monitors, the DustTrak and the E-BAM, in both the 1 min and hourly comparisons (Fig. 3a, b, respectively). Pairwise correlations among the 1 min averaged individual PUWPs raw data ($R^2 = 0.97$ – 0.98) and between the PUWPs raw data and the DustTrak ($R^2 = 0.86$ – 0.89) were high (Fig. 3a). The 1 h averaged correlations among the individual PUWPs, between the PUWPs and the DustTrak, between the PUWPs and the E-BAM, and between the DustTrak and the E-BAM were also high ($R^2 = 0.97$ – 1.00 , 0.86 – 0.89 , 0.85 – 0.90 , 0.91 , respectively). PUWP2 logged than two days of data and fewer data points resulted in a higher correlation ($R^2 = 0.97$) for PUWP2 with the DustTrak as compared with the other PUWPs.

3.3. Predictive models

Using the Bayesian information criterion (BIC) and standard error of regression (S) (Tables 2a and 2b, respectively) as indicators of model fit, a separate model was selected for each sensor using 1 min averaged DustTrak data. Fifth order polynomial models that included relative humidity (RH %) and temperature (°C) was found to best convert PUWP signals into PM_{2.5} mass concentrations. Because the correlations between the PUWPs and the DustTrak followed a sinusoidal form (Fig. 3a and b), second order models were not considered. The correlations between predicted PM_{2.5} concentrations from each PUWP after applying the model and the MiniVol-corrected DustTrak readings had R^2 ranging from 0.91 to 0.94.

When comparing models with and without relative humidity and temperature variables, models including these two variables had improved fit to the data (Tables 2a and 2b). All models had significant ($P < 0.001$) relative humidity (RH) and temperature (T) terms. Although the lowest BIC and S values were associated with sixth order polynomials, we found very small improved model fit to the data when comparing the fifth and sixth order models as measured by the decreases in BIC and S (Fig. 4a, b). Therefore, fifth order polynomial models were selected.

3.4. Distributed field deployment

Pairwise comparison between the 24 h integrated PUWP and the MiniVol data across all sites was moderate ($R^2 = 0.53$). PUWP monitors reported 24 h averaged PM_{2.5} mass concentrations that on average were 39.39 $\mu\text{g}/\text{m}^3$ lower that reported from their co-located MiniVol monitors (Fig. 5). Temperature (°C) and relative humidity (%) across the sites averaged –2.7 °C and 9.4%, respectively (Table 3). The average temperatures during the deployment phase were markedly lower than those during the calibration phase. During the field deployment, one sensor was lost (site H) and two (sites E and F) had incomplete data due to power or data logging issues. Sites with substantial missing data (Sites E and F) were not included in this analysis.

When rank ordering the sites according to mean concentrations (Table 3), the PUWPs and the MiniVols were generally both able to identify the areas with higher level of pollution, specifically identifying the High-Technology Zone (Site G) as the site with the highest average PM_{2.5} concentrations in this study. Sites varied in the number of hours per day (range: 0–13.3 h) a high concentration threshold was exceeded, which was defined as greater than or equal to one standard deviation above the daily city-wide mean calculated from the MiniVol samples across all sites (Fig. 6). The

Table 2b

Predictive models comparison using standard error of regression (S) of models. A smaller S indicates better model fit with lower values indicating smaller average distances between data points to the model's regression line. All models had significant ($P < 0.001$) relative humidity (RH %) and temperature ($T^{\circ}\text{C}$) terms. Model with lowest S is marked with an asterisk (*) for each PUWP.

Model	Standard error of regression (S), $\mu\text{g}/\text{m}^3$						
	PUWP1 (Site A)	PUWP2 (Site B)	PUWP3 (Site C)	PUWP4 (Site E)	PUWP6 (Site F)	PUWP7 (Site D)	PUWP8 (Site G)
Linear	48.89	19.25	43.72	46.65	49.85	44.90	47.95
Linear with RH and T	47.24	18.98	42.83	46.18	48.39	43.67	47.08
3rd Order Polynomial	43.20	17.72	34.86	40.50	42.97	36.01	40.95
3rd with RH and T	43.20	16.91	35.59	41.72	43.61	37.08	42.16
4th Order Polynomial	41.23	17.48	33.99	40.05	42.52	35.54	40.53
4th Order with RH and T	39.56	16.64*	33.79	38.20	39.15	34.92	36.83
5th Order Polynomial	41.23	17.48	33.87	39.98	42.52	35.54	40.51
5th Order with RH and T	39.47	16.65	33.76	38.09	38.98*	34.73	36.74*
6th Order Polynomial	41.16	17.51	34.02	39.95	42.51	35.39	40.52
6th Order with RH and T	39.46*	16.66	33.53*	38.05*	38.98*	34.65*	36.74*

PUWPs were also able to identify Site G also as the site with the most hours of concentrations considered high as compared to the rest of the city (mean: 3.97 h, range: 0.16–13.6 h) (Fig. 6). Temporally, the sites generally had similar trends with most of the extreme PM_{2.5} concentrations occurring in the early morning before 9am. However, for Site G, these extreme concentrations had a peak in the early morning and also another peak mid-day (Fig. 7).

4. Discussion

4.1. Main findings

Our main objective was to determine how the low-cost PUWP sensor would perform in areas with high PM_{2.5} levels. The 24 h averages of PM_{2.5} concentrations from the PUWPs had a moderate correlation ($R^2 = 0.53$) with their co-located MiniVol monitors. While this correlation may not seem high, when identifying potential air pollution hotspots among the sites, both the PUWPs and the MiniVols identified Site G as having the highest PM_{2.5} level. Given the cost difference between the two monitors, the PUWPs performed well and has potential to be used to rapidly screen large areas to help identify where more targeted monitoring is necessary.

Identifying the High-Technology Zone site (Site G) as a hotspot was unexpected because the area is considered to be cleaner and better planned area with more green space, lower population densities, higher property values, and higher socioeconomic status of residents. However, the high ambient PM_{2.5} levels may result from our site being close to a major road (66 m, Table 1) and the High-Technology Zone bordering western areas of Xi'an that are undergoing development and renovation. The high PM_{2.5} concentrations could be a result of the increased emissions from high polluting vehicles such as construction trucks and biomass burning that are then dispersed to the east, as the dominant wind direction in Xi'an is to the northeast.

Site G also had a different temporal pattern for its extreme values as compared to other sites. The increase in counts of extreme values in the early morning (before 9am) is most likely due to the lower mixing layer in the winter evenings and mornings. Site G's first peak in the early morning is following by another larger peak mid-day that is sustained until 4pm while other sites only had a peak in the early morning hours. While more information about sources is necessary to parse out the reasons for this trend, we can speculate that this increase is not a result of increased vehicle traffic because it does not seem correspond with traffic trends which are higher in the morning and evenings. Increased construction activity during the day from the western neighborhoods could be a potential reason.

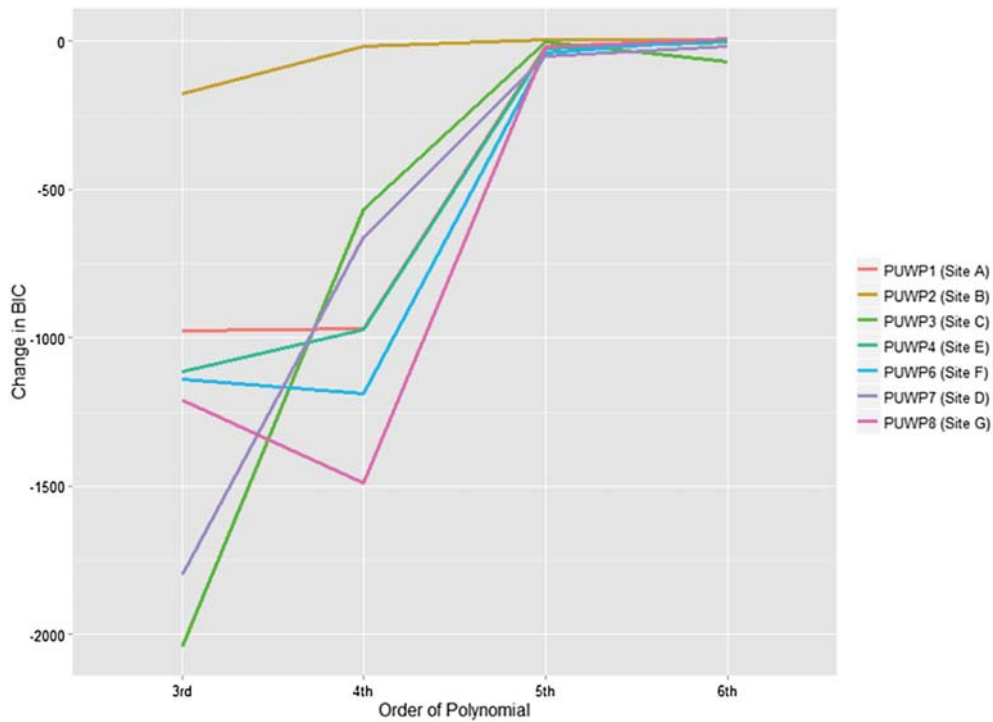
While we have identified a potential PM hotspot in this study

relative to the other sites, the 24 h health guidelines have far been exceeded across all the sites every day. Using the PUWP monitors provided insights into the temporal patterns of when extreme concentrations occur. However, the health effects of exposure to PM_{2.5} at the highly variable 1 min and 1 hourly time scale is not yet well understood. Further, health standards are not yet available for the general population at these finer time scales.

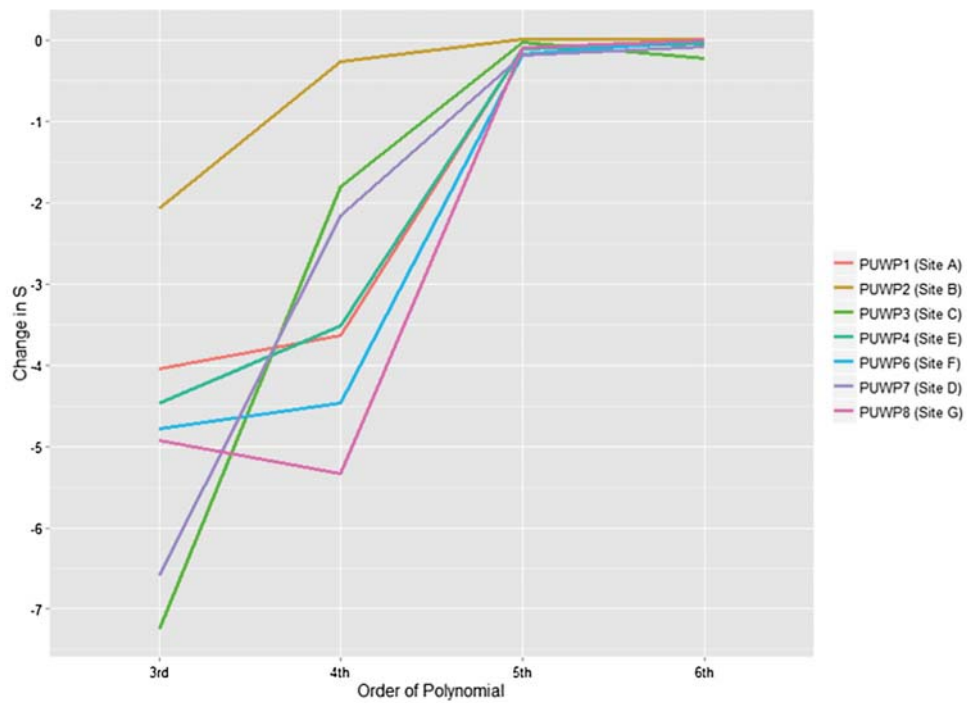
In calibrating the PUWP monitors, this study found that at high concentrations of PM_{2.5}, a fifth order polynomial model fit the data best. A previous study in the US found that the relationship was linear (Holstius et al., 2014). The difference in calibration models is most likely due to gradual saturation in the ability of the Shinyei optical sensor in the PUWPs to detect ambient concentrations above $300 \mu\text{g}/\text{m}^3$, as observed from the sinusoidal relationships (Fig. 3a). This saturation at higher concentrations is consistent with chamber studies conducted using monodispersed particles (paper forthcoming). We also observed higher pairwise correlations ($R^2 = 0.87$ – 0.89) of the PUWP monitors with the DustTrak and E-BAM than Holstius et al. did ($R^2 = 0.64$ – 0.70). We believe this is due to the larger errors in detection at the low concentrations, as shown in the Shinyei's manufacturing specification sheet (Shinyei Corp. 2010). Because the concentrations at the US site are lower than the ones in this paper, we would expect lower R^2 values at lower ambient concentrations.

In addition, the standard error of regression (S) averaged $34 \mu\text{g}/\text{m}^3$ across the PUWPs between the predicted PM_{2.5} values estimated by the 5th order polynomial models and the corresponding 1 min DustTrak concentrations (average of $328.3 \mu\text{g}/\text{m}^3$). This 10% measurement error can be expected because we created the models using nosier 1 min DustTrak data. We would expect this error to be lower had we used 1 h averaged data. As expected, in Holstius et al., the measurement error was found to be 1–10 $\mu\text{g}/\text{m}^3$ based on hourly PM_{2.5} data. The magnitude of measurement error depends on the time resolution selected of the reference instruments and suggests tradeoffs between precision and temporal resolution should be considered based on the purpose of the study.

Finally, this study found significant effects from relative humidity and temperature in the predictive models while these variables were found to be insignificant previously. This difference in findings could result from differences in meteorological conditions between the spring and summer seasons. This study's December mean temperatures and relative humidity were lower than those in the US study which was conducted in April and had slightly larger diurnal temperature changes and less variability in relative humidity (approximately range of 3–17% versus range of 10–60%). The significance of relative humidity and temperature in this study is most likely due to the diurnal trends of these two variables correlating with time of day, which plays a larger role in



(a)



(b)

Fig. 4. Diminishing returns in improved model fit as measured by changes in (a) BIC and (b) S with increasing model complexity when comparing models (linear, third, fourth, fifth, and sixth order polynomials) that include relative humidity (RH) and temperature (T). A lower BIC when comparing two models for the same data indicates a better fitting model while accounting for complexity of the model. A smaller S indicates better model fit with smaller values indicating smaller average distances between data points to the model's regression line.

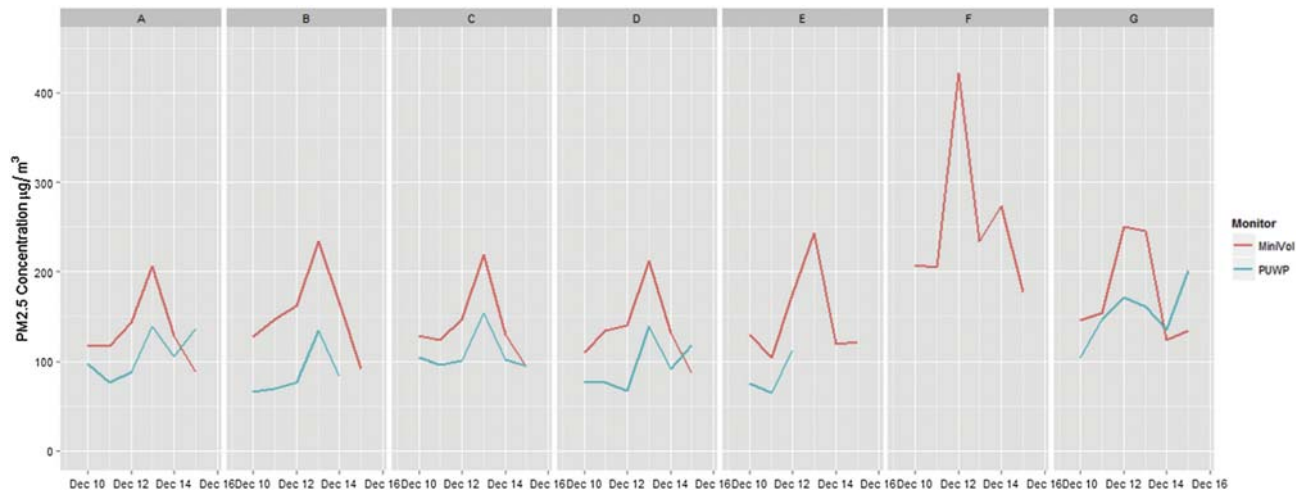


Fig. 5. PUWP monitor compared to co-located MiniVol 24 h PM2.5 concentrations across distributed deployment sites. Sites B, E, and F had missing data that prevented calculation of complete 24 h PM2.5 data.

Table 3
Distributed field deployment 24 h averaged site summary statistics.

Site	PUWP ($\mu\text{g}/\text{m}^3$)		MiniVol ($\mu\text{g}/\text{m}^3$)		Relative humidity (%)		Temperature ($^{\circ}\text{C}$)	
	Mean	SD	Mean	SD	Mean	SD	Mean	SD
A	106.90	25.72	133.67	40.21	10.56	1.88	-3.88	2.97
B	85.91	27.91	154.63	47.64	9.00	3.49	-2.86	4.03
C	108.47	22.66	140.16	42.08	9.47	3.67	-3.44	3.99
D	84.06	27.93	133.67	42.34	9.29	2.65	-2.20	3.51
E	Incomplete data		148.83	51.92			Incomplete data	
F	Incomplete data		253.04	88.70			Incomplete data	
G	153.23	32.99	175.60	56.91	9.68	5.07	-1.38	5.76
H	Sensor lost		134.51	37.39			Sensor lost	

determining PM concentration in this study. The inversion layer during the winter is more pronounced and has a diurnal pattern, resulting in concentrating PM by preventing particle dispersion at night and in the early mornings. Therefore, relative humidity and temperature were found to be significantly associated with PM2.5

concentrations in this winter study.

4.2. Limitations

The findings that indicate the usefulness of low-cost PM monitoring at higher ambient concentrations in Xi'an were comparable to the ones found in a collocation study conducted in the United States (Holstius et al., 2014). However, the detection of a saturation point in the field, as also observed in chamber studies (paper forthcoming), requires more work to understand the technological limitations of the device and environmental parameters under which these PUWPs can be used. In addition, studies thus far have not examined the effects of different optical and chemical PM2.5 compositions, seasonal variation, and meteorological conditions (e.g., temperature, precipitation, and relative humidity) on PUWP detection and calibration. More tests are needed to understand how variability in PM composition can change the PUWP monitor's performance. While fifth order polynomials were determined to be the best fitting for this Xi'an study, this same model may not

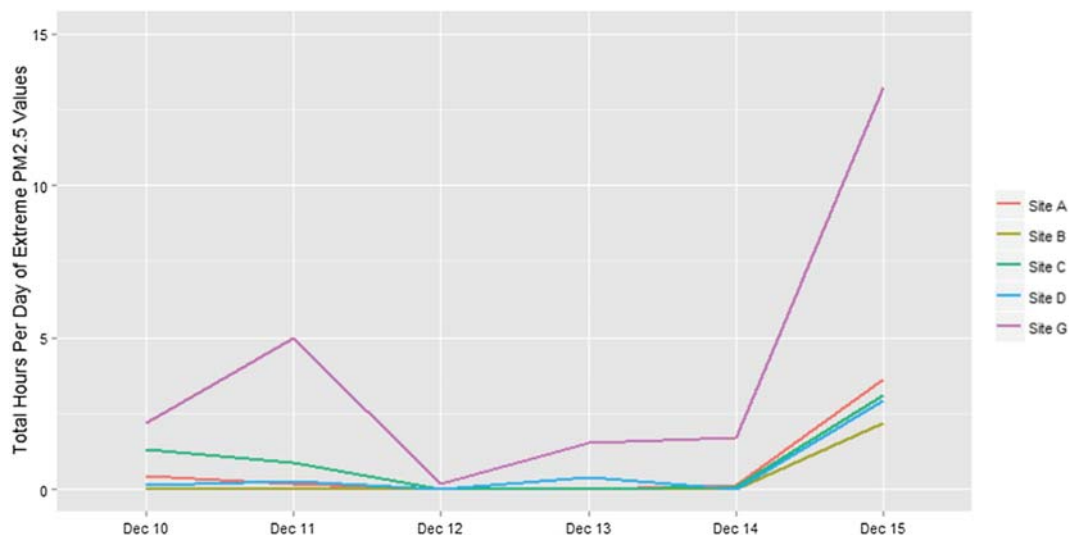


Fig. 6. Total hours per day where mass concentrations of PUWPs exceeded one standard deviation above the daily city-wide average (as calculated from the mean of the MiniVol samples from all sites).

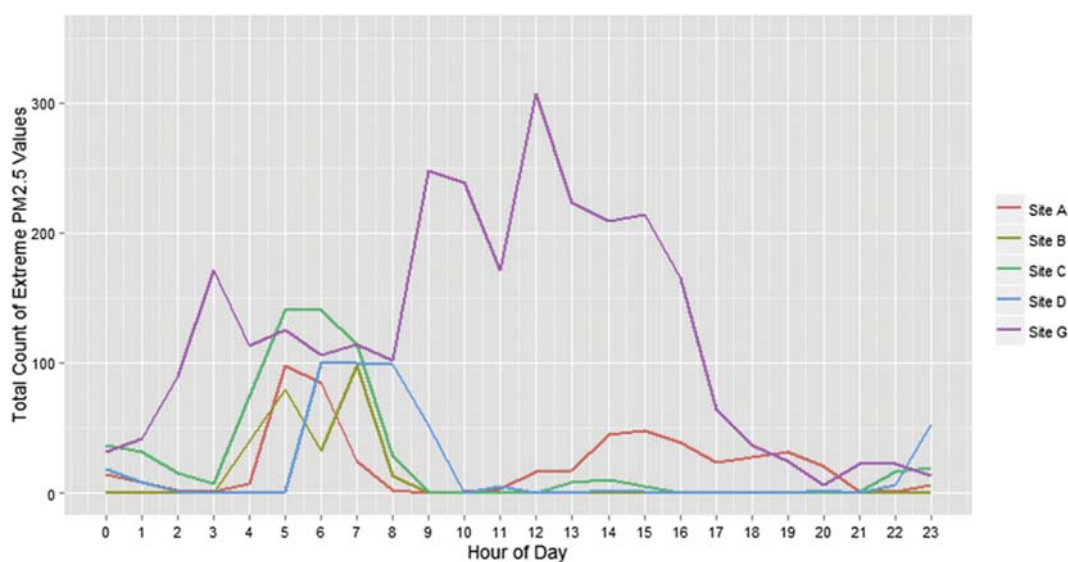


Fig. 7. Daily temporal variation of high PM_{2.5} mass concentrations from PUWP monitors across the sites over the days sampled showing the count of 1 min averaged samples where mass concentrations exceeded one standard deviation above the daily city-wide average.

necessarily hold in another location. Presently, new calibrations must be conducted prior to any field deployment in new study sites and more studies should be conducted under different seasonal and environmental conditions to test how well this calibration model holds.

In addition, we selected Site G as our calibration site but the aerosol composition, optical properties, and size distribution at one site could differ from that of other sampled sites around the city. While resource limitations prevented us from creating calibration curves specific to each sampling site in this pilot study, we believe using one local site for calibration is an improvement over using pre-existing calibration data. In some research applications, the use of less accurate lower cost sensors to estimate exposure for a population over a large area may outweigh the benefits of using a few more accurate but expensive instruments.

In the current study, because we were primarily interested in calibrating the PUWPs at all deployment sites, they were co-located with reference instruments. In future studies, once co-location of the PUWPs at a single regionally representative site, and the relationships between the PUWPs sensors and a reference instrument like the E-BAM or DustTrak is observed, a large number of PUWPs can be distributed across a city. Given the low cost of the sensor (\$15 USD) and of each PUWP monitor (<\$500 USD) which is several orders of magnitude lower than that of the E-BAM or DustTrak, such large deployments considerably more cost-effective than deploying traditional gravimetric samplers like the MiniVols. Moreover, because the instruments are optical and continuous logging, they require less field staff involvement compared to filter pre and post-weighing, and exchange of filters every 24 h as necessitated by gravimetric methods. These future deployments could be focused in city regions where we have initially identified relatively high concentrations (e.g., the High-technology Zone region G in Xi'an) to better understand PM sources, secondary aerosol formation, dispersion, and population exposures. This hierarchical approach of city-wide screening, followed by more spatially dense deployments in hotspots is made easier by the fact that the instruments are low-cost and highly portable, and can lead to increasingly focused monitoring important emission and population exposure areas of the urban environment.

Additionally, more affordable direct-reading monitors like the

PUWPs can be used to enhance air pollutant exposure assessments through land-use regression (LUR) (Briggs et al., 1997), where sampling is often conducted in short campaigns in select seasons of the year to represent seasonal or annual averages, but limited to no temporally-resolved data are available to inform how concentrations vary on finer spatial and temporal scales. This lack of data limits the LUR models' ability to identify hotspots for use in regulatory applications where emissions and resulting population exposures vary temporally (e.g., on the order of minutes to hours). The combination of spatially and temporally resolved data available from PUWPs could potentially solve these problems for future health effects and air quality management studies.

5. Conclusions

This study demonstrated that the PUWP monitors could be used to enhance existing PM_{2.5} sampling networks and for use in health-related studies as an affordable technology to increase spatiotemporal resolution of PM_{2.5} datasets, both in ambient monitoring networks and even in higher PM_{2.5} conditions for rapid screening. Although additional calibration studies under varying meteorological conditions in different regions would be useful, the PUWPs show promise as a viable lower cost aerosol sensor that can be used in developing or industrializing area applications where obtaining expensive instrumentation to monitor air quality can be costly but where the need for monitoring is especially urgent to protect public health.

Acknowledgments

This research was funded by the University of California Berkeley Wood-Calvert Chair grant and the United States Fulbright Program. Funding for the PUWP monitors was provided by Department of Environmental & Occupational Health Sciences at the University of Washington.

References

- Briggs, David, Collins, Susan, Elliott, Paul, Fischer, Paul, Kingham, Simon, Lebet, Erik, Pryn, Karel, van Reeuwijk, Hans, Smallbone, Kirsty, van der Veen, Andre, 1997. Mapping urban air pollution using GIS: a regression-based

- approach. *Int. J. Geogr. Inf. Sci.* 11 (7), 699–718. <http://dx.doi.org/10.1080/136588197242158>.
- Cao, Junji, 2014. Chapter 5 我国PM2.5研究综述 (Characterization of China's PM2.5). In: *PM2.5与环境 (PM2.5 and the Environment in China)*. Science Press LLC.
- Holstius, D.M., Pillarisetti, A., Smith, K.R., Seto, E., 2014. Field calibrations of a low-cost aerosol sensor at a regulatory monitoring site in California. *Atmos. Meas. Tech. Discuss.* 7 (1), 605–632. <http://dx.doi.org/10.5194/amtd-7-605-2014>.
- Kan, Haidong, Chen, Renjie, Tong, Shilu, 2012. Ambient air pollution, climate change, and population health in China. *Environ. Int.* 42 (July), 10–19. <http://dx.doi.org/10.1016/j.envint.2011.03.003>.
- Shinyei Corp, 2010. Specification Sheet of Particle Sensor Model PPD42NS. Available at: <http://www.sca-shinyei.com/pdf/PPD42NS.pdf> (last accessed 20.01.15.).
- Statistical Bureau of Shaanxi Province, 2010. Shaanxi Statistical Yearbook 2010. www.chinadataonline.org.
- US EPA, 2012. National ambient air quality standards for particulate matter: final rule. *Fed. Regist.* 78 (10). Part II: 40 CFR Parts 50, 51, 52 et al.
- World Health Organization, 2005. WHO Air Quality Guidelines Global Update 2005: Report on a Working Group Meeting, 18–20 October 2005. World Health Organization, Bonn, Germany. <http://apps.who.int/iris/handle/10665/79170>.
- Yang, Gonghuan, Wang, Yu, Zeng, Yixin, Gao, George F., Liang, Xiaofeng, Zhou, Maigeng, Wan, Xia, et al., 2013. Rapid health transition in China, 1990–2010: findings from the global Burden of disease study 2010. *Lancet* 381 (9882), 1987–2015. [http://dx.doi.org/10.1016/S0140-6736\(13\)61097-1](http://dx.doi.org/10.1016/S0140-6736(13)61097-1).